INDIAN JOURNAL OF SCIENCE AND TECHNOLOGY

ORIGINAL ARTICLE

Brain Cerebrospinal Fluid variation in Dementia using Radiomic Features and Optimized Machine Learning Techniques

Ahana Priyanka[1]*, A. R. Jac Fredo[2], Kavitha Ganesan[3]

1 Department of Computer science & Engineering, Sri Sivasubramaniya Nadar College of Engineering, Chennai, 603110, Tamil Nadu, India
2 School of Bio-Medical Engineering, Indian Institute of Technology (BHU), Varanasi 221005, Uttar Pradesh, India
3 Department of Biomedical Engineering, CEG Campus, Anna University, Chennai, Tamilnadu 600025, INDIA

OPEN ACCESS

Received: 28/01/2025
Accepted: 07/11/2025
Published: 01/12/2025

Citation: Priyanka A, Jac Fredo AR, Ganesan K (2025) Brain Cerebrospinal Fluid variation in Dementia using Radiomic Features and Optimized Machine Learning Techniques. Indian Journal of Science and Technology 18(43): 3406-3421. https://doi.org/10.17485/IJST/v18i43.194

* **Corresponding author**.

ahanachellian@gmail.com

Funding: None

Competing Interests: None

Published By Indian Society for Education and Environment (iSee)

ISSN
Print: 0974-6846
Electronic: 0974-5645

Abstract

Objective: Dementia causes degeneration of neurons in brain. This disorder prognosis is difficult to understand in a non-invasive manner. This study is an attempt to understand CSF texture variations across different dementia severity stages using optimized machine learning model. Since this biomarker has not been fully explored for different severity changes of brain diseases. **Methods:** In this study, ADNI database is considered to attain normal (HC), EMCI, MCI, LMCI and AD images. The skull stripped images are segmented using multilevel Tsallis based moth flame optimization. Further, GLCM, ZM, LBP, ST and PHOG features are extracted to study pathological texture variation in CSF. Multi-subspace randomization and collaboration (MSRC) based feature selection method is used to attain significant feature. Finally, SVM performs multiclass classification. **Findings:** Results indicate that the proposed method precisely segmented CSF region for all considered images with high correlation values of 0.9. The MSRC method identifies appropriate rank for the considered feature vectors based on the performance in multiple subspaces. ANOVA test identifies optimal features set with a p-value < 0.001 for classification. It is noticed that SVM classifier classify HC (99%) , EMCI (97%), MCI (96%), LMCI (98%) and AD (96.1%) images with better prediction. **Novelty:** The novelty of this work is to integrate optimized thresholding model, texture analysis, and statistical validation to establish a measurable link between CSF biomarkers and dementia severity stages. Hence, it could offer better clinical insights for clinicians to make appropriate decisions regarding the progression of dementia severity stages and its underlying changes.

Keywords: Dementia; Cerebrospinal fluid (CSF); Moth flame optimization; Texture feature; Multi-subspace randomization and collaboration (MSRC)

1 Introduction

Dementia is an irreversible neurodegenerative disorder characterized by progressive cognitive decline. It causes gradual neuronal loss, leading to structural and functional abnormalities in cortical regions[1]. According to Alzheimer's Disease International, approximately 47 million people worldwide are affected by dementia[2]. The common symptomatic stages include early mild cognitive impairment (EMCI), mild cognitive impairment (MCI), late mild cognitive impairment (LMCI), and Alzheimer's disease (AD), which are primarily identified through cognitive assessments. However, no specific symptom can consistently determine the progression of dementia, as brain alterations often occur before the appearance of amnestic symptoms[3].

Research on neurodegeneration focuses on the role of abnormal amyloid-beta accumulation in cerebrospinal fluid (CSF) during the early stages[4]. However, CSF remains a sparsely studied region despite its established implication in dementia progression, especially when compared to regions such as the hippocampus, corpus callosum, and lateral ventricles[5]. Changes in CSF are closely linked to the neurochemical environment and can reflect subtle alterations in the brain even before they become clinically apparent. These alterations may influence the texture and volume of CSF, as neuronal degeneration affects surrounding tissue structures[6]. By examining these subtle textural variations in CSF, this work aims to uncover early neurodegenerative changes that contribute to dementia prognosis. Previous studies suggest that such inevitable texture changes associated with neurodegeneration can be effectively captured using structural magnetic resonance (MR) imaging[1]. This study addresses the existing research gap by focusing not only on CSF volume but also on texture variations arising from brain atrophy, which alter CSF fluid dynamics and composition. These subtle variations can be quantified through MR imaging, positioning CSF as a crucial biomarker. Thus, this work leverages the potential of CSF to detect early-stage changes that may be overlooked by other biomarkers. However, direct analysis of CSF may not be sufficient to reveal progressive changes using structural MR alone; such variations can be better identified through pattern recognition and machine learning techniques.

Segmentation of the CSF region presents several challenges due to its complex orientation and morphological associations with surrounding tissues[3]. Both automatic and semi-automatic segmentation methods can be considered for such complex delineations. Methods like FreeSurfer and FSL primarily estimate CSF volume, but they require extensive hyperparameter tuning, which can be difficult for intra-class subject delineations. Similarly, Level Set methods are often complex in identifying boundaries in abnormal images due to geometric variations[4]. Region growing techniques tend to be sensitive to noise and the choice of initial seed, which may lead to over-segmentation or under-segmentation, particularly in pathological cases. Watershed segmentation performs well when image boundaries are clearly defined, but it struggles in the presence of noise or poorly contrasted regions. Deep learning-based CSF segmentation approaches may sometimes misinterpret background structures as relevant features, leading to inaccuracies during training and requiring substantial computational resources. Therefore, this study employs a thresholding-based approach that distinguishes different gray-level intensities in an image[7]. Specifically, Tsallis entropy is utilized to capture the maximum probability of gray-level variations suitable for multilevel thresholding. The Moth Flame Optimizer (MFO) is then used to determine the optimal thresholds without structural adjustments to the algorithm, owing to its intrinsic search ability, flexibility, and gradient-free nature[8]. This approach effectively preserves CSF structure, which is crucial for accurately delineating abnormal MR images.

Literature shows that texture features extracted from MR images are used to provide quantitative information about the region of interest rather than its atrophy rates which are suitable to observe diagnostic differences[9]. Conventional texture features such as grey level co-occurrence matrix (GLCM), structure tensor (ST), Zernike moments (ZM), local binary pattern (LBP) and pyramid histogram of gradient (PHOG) have been extracted from the segmented CSF region. These features help to reveal the subtle invisible texture abnormalities that are accumulated in CSF[1]. Further, these measures provide morphological information which is found to be robust to identify the variations in CSF that correlate with amyloid degeneration. These features could help to better understand disease progression and early diagnosis, offering advantages over traditional atrophy measurements and functional brain changes in disease prognosis.

Further, to improve the diagnostic prediction and prognostic information obtained from extracted textures, feature selection is performed. Generally, feature ranking methods are considered in feature selection to handle the high-dimensional texture features, as they are computationally inexpensive. Methods such as mutual information, genetic algorithms, and recursive feature elimination have several limitations when applied to CSF features, including the tendency to capture redundant features, inefficiency in handling correlated features, and susceptibility to overfitting[1]. This study uses the multi-subspace randomization and collaboration (MSRC) technique for ranking the features. This method considers features in different subspaces and ranks them based on their performance, resulting in a robust and interpretable feature set[10]. The ranked features have a high degree of significance and efficiently improve the performance of classification. Methods such as clustering are sensitive to initial centroid placements, voting is dependent on the performance of individual base models, and deep learning models require large amounts of labeled data. However, SVM ability to prevent overfitting through regularization and its

strength in handling non-linear boundaries through the kernel trick make it optimal for predicting the severity prognosis of CSF[6]. Its efficacy lies in its fault tolerance and better generalization.

This study attempted to investigate the progression of dementia stages in CSF. The work focuses on textural variations of CSF in healthy control (HC), EMCI, MCI, LMCI and AD images. Multilevel Tsallis based MFO is considered for segmentation. Various texture features are extracted from the segmented region which gives spatial and gradient information with distinct moment in different directions. Significant feature is selected using MSRC and analysed. SVM based classification is carried out on these features and clinical correlation is performed.

The main contributions of this study are as follows:

- Precise segmentation of the CSF region in normal, EMCI, MCI, LMCI, and AD stages using multilevel Tsallis entropy-based MFO.
- Analysis of the variations in texture features of the CSF region across the different disease stages to assist in disease prognosis.
- Identification of significant features using the MSRC method, followed by statistical testing.
- Classification of normal, EMCI, MCI, LMCI, and AD stages based on texture features extracted from the CSF region.

2 Methodology

The workflow is depicted in Figure 1. The T1 weighted trans-axial view MR images of 2500 from HC, EMCI, MCI, LMCI and AD subjects are considered from a public database ADNI based on cognitive scores. The images are pre-processed using robust brain extraction tool. CSF is segmented using multilevel Tsallis based MFO. GLCM, ST, ZM, PHOG and LBP features are extracted from segmented CSF to observe the texture difference. Further, MSRC method selects discriminative features based on ranking. Finally, classification is carried out with the help of multiclass SVM. Finally, significant texture feature is correlate with clinical score. Thus, CSF is found to demarcate the clinical pathology of the severity levels.

2.1 Image Database

Alzheimer's Disease Neuroimaging Initiative (ADNI) database (https://adni.loni.usc.edu/) images was used in this study[11]. The current study utilized data from the ADNI-1 and ADNI-2 cohorts. ADNI-1 primarily includes baseline scans, while ADNI-2 provides both baseline and follow-up data and introduces further subclassification of MCI into EMCI and LMCI groups. In this work, we considered only the baseline scans of the selected subjects to maintain consistency in disease stage representation and avoid longitudinal variability. The mean age ($\pm$ standard deviation) for each group was: HC (75.8 $\pm$ 5.0), EMCI (74.8 $\pm$ 6.9), MCI (74.7 $\pm$ 7.5), LMCI (75.0 $\pm$ 7.7), and AD (75.3 $\pm$ 7.3). The severity of the subjects was categorized based on cognitive examination. However, this examination is only suitable for preliminary analysis[12]. In order to reveal prognostic information T1 weighted MR image is considered.

A total of 150 subjects were selected from each class such HC, EMCI, MCI, LMCI, and AD resulting in 750 subjects overall. From these, 500 representative middle slices were extracted per class (500*5 = 2,500 total images). Middle slices were chosen as they capture the most prominent anatomical variations in the CSF regions. The image slice positions for each subject were determined independently. From each subject, two or three middle slices from the T1-weighted MRI were selected to represent the cerebrospinal fluid (CSF) region. Since middle slices often exhibit structural variations associated with neurodegenerative disorders, the images were carefully selected based on visual evaluation criteria.

2.2 Pre-processing

The morphometric studies of MR brain images often require pre-processing. This phase delineates extra cranial tissues from the images[13]. This framework adopts robust learning- based brain extraction tool (ROBEX) for delineation of non-brain tissues[14]. This method is trained with various brain templates for exact delineation of brain mask. Point distribution and deformation model are used in the method which balances the variation in brain shape. This helps to preserve the prominent brain regions that are highly influential in cognitive impairment.

2.3 Multilevel Tsallis based moth flame optimization

Initially, skull stripped images are segmented then CSF is extracted from brain tissue to capture the changes for normal and abnormal images[15]. Tsallis entropy based multilevel thresholding is attempted to measure the distinct information content in an image. This entropy becomes complex when number of thresholds increases. Hence, optimizer is adopted. The optimizer

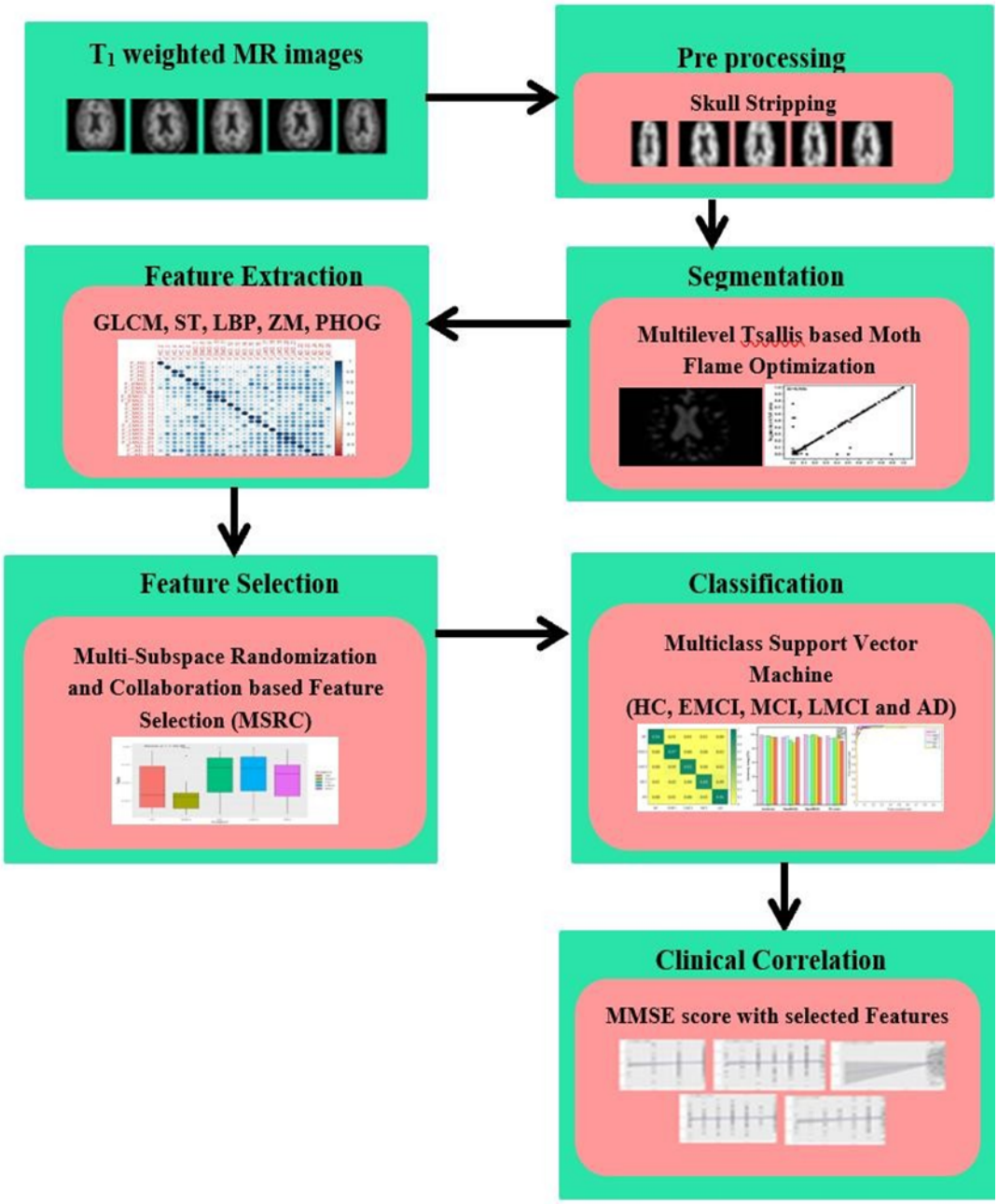

Fig 1. Work flow of the proposed study

influences the objective function of Tsallis entropy which gives optimal thresholds. This is expressed as[16],

$$T_{opt} = \arg max\left[S^p(t) + S^q(t) + (1-x)\cdot S^p(t)\cdot S^q(t)\right] \quad (1)$$

Here t is the number of thresholds values x determine the degree of non-extensivity in an image. Further, moth flame optimization (MFO) is adopted to optimize the thresholds. This is a population-based optimizer which works based on navigating mechanism of moths called transverse orientation. Moth and flames are initialized in the search space. Flame refers to the artificial light of the moth. The optimized thresholds are obtained by best visited position of each moth towards flame. It is denoted as[8],

$$S\left(E_i, F_j\right) = Z_i \cdot e^{bt} \cdot \cos(2\pi t) + F_j \quad (2)$$

Here, Ei represents i^{th} moth and Fj denotes the j^{th} flame. Zi indicates the distance between jth flame and i^{th} moth, t represents a random number in [-1, 1] and b is a constant that indicates the shape of the logarithmic spiral. Thus, the optimizer provides high exploitation capability and has the ability to optimize search spaces with infeasible regions[17]. Thus, this characteristic is useful to identify optimum thresholds in brain to segment the appropriate region.

2.4 Texture Feature

The texture features are extracted from the segmented CSF to examine the prognosis variation in an image. Initially, GLCM matrices are used to calculate statistical and correlation measures from heterogeneous image[18]. This feature helps to infer the occurrence of pixel pair and spatial relationship between the pixels. Thus, local pattern of GLCM features are constructed. Consequently, LBP descriptor extracts the local information of each pixel based on joint distribution difference with neighbourhood pixels[19]. Further, ZM are obtained by projecting the image in a complex orthogonal polynomial[20]. This polynomial descriptor uses various moments with corresponding repetition order to generate feature information. The higher and lower order moments describe the different global details of an image. Subsequently, in PHOG canny edge is extracted for an image and is divided into spatial grids and orientation gradients are computed using sobel mask[20]. Finally, the gradients of each grid are linked together at each pyramid level. Thus, local and global based orient gradient information are extracted. Lastly, ST captures the local dimensionality and the corresponding orientation for simple neighborhoods in an image[21]. It shows the similarities and prominent orientations of image gradients. It analyses the major directions of the gradient in a definite neighborhood of a point, and the degree to which those directions are coherent. Thus, these features have been applied in various medical image detection and classification. Finally, this study utilises the property of each feature to capture the microstructural information and identify texture alterations.

2.5 Feature Selection

The extracted texture features are given to multi-subspace randomization and collaboration (MSRC) based feature selection method[10]. Initially, each feature is participated in a multiple sub-space[22]. Each sub-space holds diverse and balanced features with similar size. Further, these features construct KNN graph with appropriate structure. Based on the graph, Laplacian analysis is carried out and a Laplacian score is obtained for each feature that holds their performance. Finally, feature vector with score for multiple sub-space are concatenated. These feature vectors are ranked based on averaging the performance of each feature. Further, analysis of variance (ANOVA) test is carried out to understand the influence of considered features[6]. Thus, this method improves the distinctive capability of the classifier between classes, speeds the classification task and reduces the computational time.

2.6 Classification

Support vector machine (SVM) is widely attempted to classify the variations in medical images. Here each feature is considered as a point in N-dimensional space with the value of each feature being the value of a particular coordinate[23]. Then classifier discriminates the classes based on hyper plane[24]. This plane is created among the classes that represent the longest distance between closest data points. The tuning of parameters such as gamma (γ) and constant C highly influences the plane. Finally, performances measures are obtained as classification result[25].

3 Results of the Proposed Work

3.1 Analysis of pipeline

The typical T1 weighted MR images of HC, EMCI, MCI, LMCI and AD in trans-axial view are shown in Figure 2(a-e). The structure of brain regions differs in normal and abnormal images. These changes are reflected in CSF which is accountable for dementia. The corresponding skull striped images are shown in Figure 2(f-j). It is visualized that delineation of non-brain tissues using ROBEX does not affect the structure of brain which pose inhomogeneious intensity, irregular tissue and edges. Hence, CSF segmentation is tedious. In order to overcome this challenging task, segmentation of CSF is achieved using multilevel Tsallis based MFO with optimized threshold which are shown in Figure 2(k-o).

3.2 Significance and impact of segmentation method

The optimized threshold is attained using the social behavior of moths. The parameters considered to optimize the threshold include the population of moths (N = 30), iterations (I = 500), and variable dimension (D = 4). The desired tuning of these

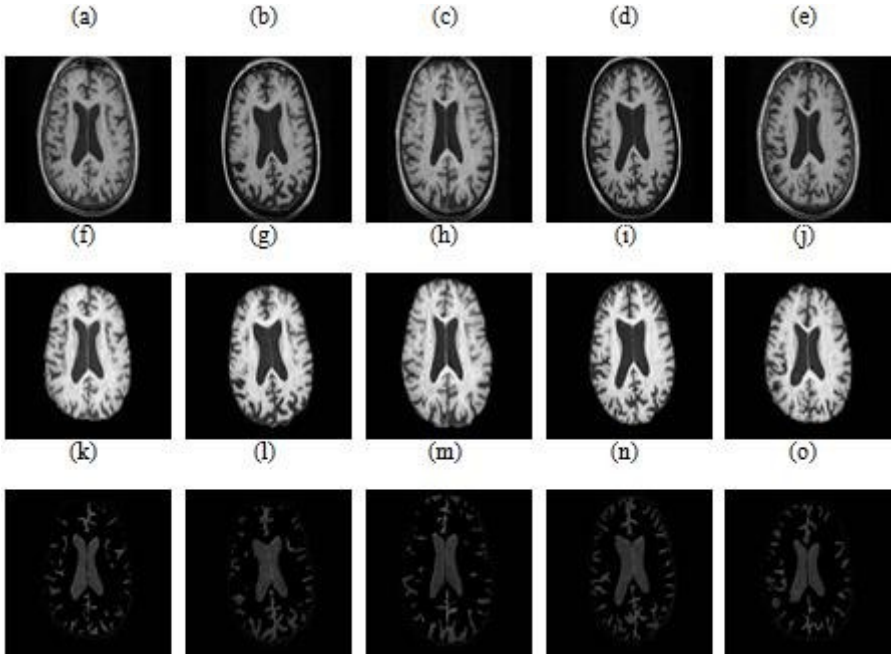

Fig 2. Typical original T1 weighted image of (a) HC, (b) EMCI, (c) MCI, (d) LMCI and (e) AD, (f-j) corresponding skull stripped images, (k-o) corresponding CSF segmented images

parameters helps to attain an appropriate threshold position to segment CSF. The extracted CSF region appears dark gray. However, the visual result of the segmented CSF structures does not provide any significant insight for discriminating different classes.

The segmentation result is quantitatively validated using the correlation measure. The correlation plots between the segmented CSF area and its corresponding gold standard area in HC, EMCI, MCI, LMCI, and AD are shown in Figure 3(a–e), extracted using the Clinical Neuroimaging Software Suite tool under expert guidance for all considered classes. The correlation value (R) of the segmented CSF is found to be above 0.9 in all the considered cases.

Further, segmentation methods are evaluated with various overlap measures with the obtained ground truth. The Dice coefficient is used to validate the degree of correspondence between the ground truth and the segmented region. Using Multilevel Tsallis-based entropy with the MFO method, the Dice coefficient is attained as HC (0.987), EMCI (0.995), MCI (0.983), LMCI (0.975), and AD (0.970), respectively. Likewise, the Jaccard index shows values of 0.974, 0.985, 0.966, 0.951, and 0.942 for HC, EMCI, MCI, LMCI, and AD images, respectively.

Consequently, CNN-based segmentation is attempted to delineate CSF from the considered images. These methods are prone to overfitting and often demonstrate poor generalization across images. Furthermore, their segmentation accuracy tends to vary with tissue type and structure complexity. The target biomarker, such as CSF segmentation, involves irregular boundaries and subtle intensity transitions. CNNs rely heavily on large-scale spatial context, which limits their adaptability. In contrast, the proposed Multilevel Tsallis Entropy + MFO approach directly utilizes the pixel-level intensity distribution and adaptively determines optimal thresholds for complex CSF structures.

From Table 1, it is shown that this approach achieves desired stable performance due to its balanced exploration–exploitation mechanism, allowing precise segmentation of complex CSF structures while preserving boundary, shape, and appearance across all severity stages. Overall, the MFO-based method effectively captures fine gray-level variations, enabling precise spatial representation of disease-related changes in each stage of MR images. Therefore, the MFO-segmented CSF regions provide meaningful features for subsequent analysis across HC, EMCI, MCI, LMCI, and AD stages.

3.3 Robustness of texture features extraction

Initially, the GLCM texture feature calculates the pixel intensities at each position of an image with the desired distance and various orientations such as 0°, 45°, 90°, and 135°. Hence, it infers 22 features that describe the spatial relationship between

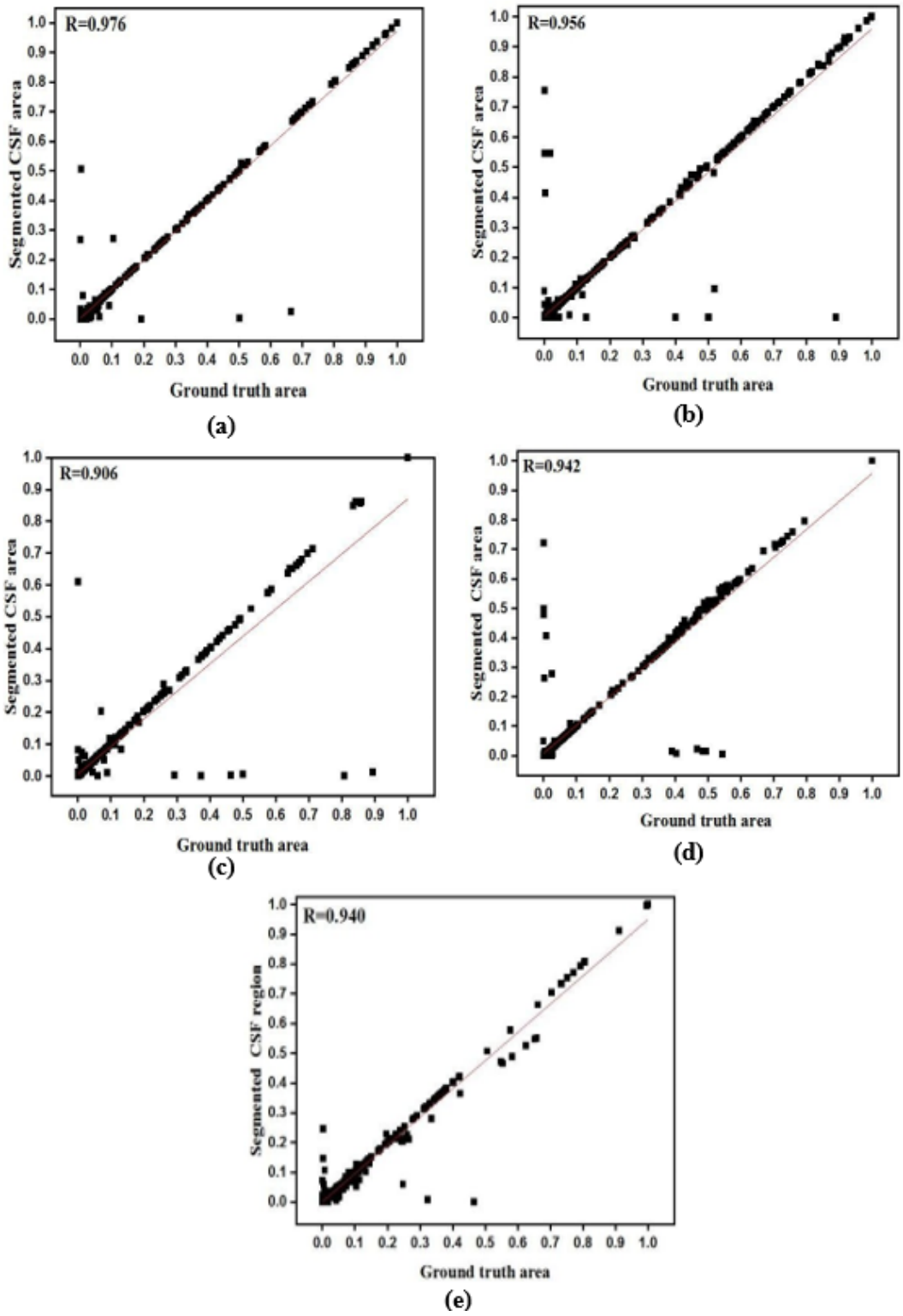

Fig 3. The correlation between segmented and gold standard CSF area for all the subjects (a) HC, (b) EMCI, (c) MCI, (d) LMCI and (e) AD

Table 1. Comparison of CSF segmentation methods on T1-weighted MR images

Method	Type	Average Dice Coefficent	Computation Time per 3D Volume	Hard-ware
Deep CNN Segmentation	Supervised learning-based segmentation	0.883	20 minutes	GPU
Proposed Multilevel Tsallis Entropy + MFO	Optimization-based thresholding	**0.982**	**8 minutes**	CPU

grey-level pixel pairs in the image. Similarly, the LBP feature creates a binary value for each pixel by comparing the center pixel with its neighbouring pixels within a 3×3 radius. Thus, 59 LBP features are obtained.

The ZM descriptor generates an intensity function using a polynomial representation of the image in space with repetition m and order n. This orthogonal projection helps to generate 25 independent features with minimal overlap. PHOG extracts local variations in an image using spatial patterns. In this study, a bin size of 8, pyramid level of 3, and orientation of 360° are considered to extract 680 features. ST computes partial derivatives and forms the Jacobian matrix using gradient information to calculate 6 features from an image.

In total, these 792 features help to identify altered CSF variations, providing insight into significant differences. Each specific texture feature is normalized to 1. Normalization transforms an n-dimensional grayscale image with intensity values (I) in the range (Min, Max) into a new image with intensity values in the range ($newmin$, $newmax$).

3.4 Analysis of MSRC method on HC and severity cases based on CSF texture features

Further, to extract prominent texture features, the MSRC method is attempted. This method selects effective texture features based on the desired performance of each feature in various sub-spaces and gives rank to each feature vector. Based on the rank, significant features are independently identified. Further, to observe the prominence nature of the obtained features, a correlogram plot is depicted. Figures 4(a) and (b) show the sample of the whole set of extracted features and the top-ranked features using MSRC for HC and severity classes, respectively. **Figure 4(b)** shows that each feature has desired information about the prognosis stages and shows distinct correlation compared to the whole set features. Thus, the MSRC method is able to rank the most relevant features based on their independent performance in various high-dimensional sub-spaces. These ranked features are able to capture the relative pixel changes in an image effectively. These substantial texture changes in pixels might occur due to anatomical changes of CSF.

The utilized method is compared against widely benchmarked methods such as Least Absolute Shrinkage and Selection Operator (LASSO), Mutual Information (MI) ranking, and Recursive Feature Elimination (RFE). Each method's significant features are utilized for feature stability comparison using the Jaccard Similarity Index (JI). This index evaluates the consistency of the selected features across repeated subsampling. The final stability score is obtained as the mean of all pairwise Jaccard indices computed over 10 independent resamplings. The performance and stability comparison of feature selection methods are summarized in Table 2. The result indicates that MSRC-based features could help to discriminate the degree of severity effectively.

Table 2. Performance comparison of feature selection methods and their stability score

Feature Selection Methods	Significant feature stability score
LASSO	0.68
Mutual Information (MI)	0.61
RFE	0.74
MSRC (Proposed)	**0.82**

3.5 Statistical analysis of MSRC method for HC and severity cases of CSF texture features

Further, efficacy of extracted texture features for HC, EMCI, MCI, LMCI and AD images are evaluated statistically. ANOVA test is carried out for MSRC feature vector and whole set. This test is carried out to understand the significant texture variation among the HC and severity classes. Figure 5(a) with whole set of feature vector shows less significance (p=0.69) in features among HC and severity class. However, Figure 5(b) depicts that MSRC based feature vector exhibits a high significant p-value.

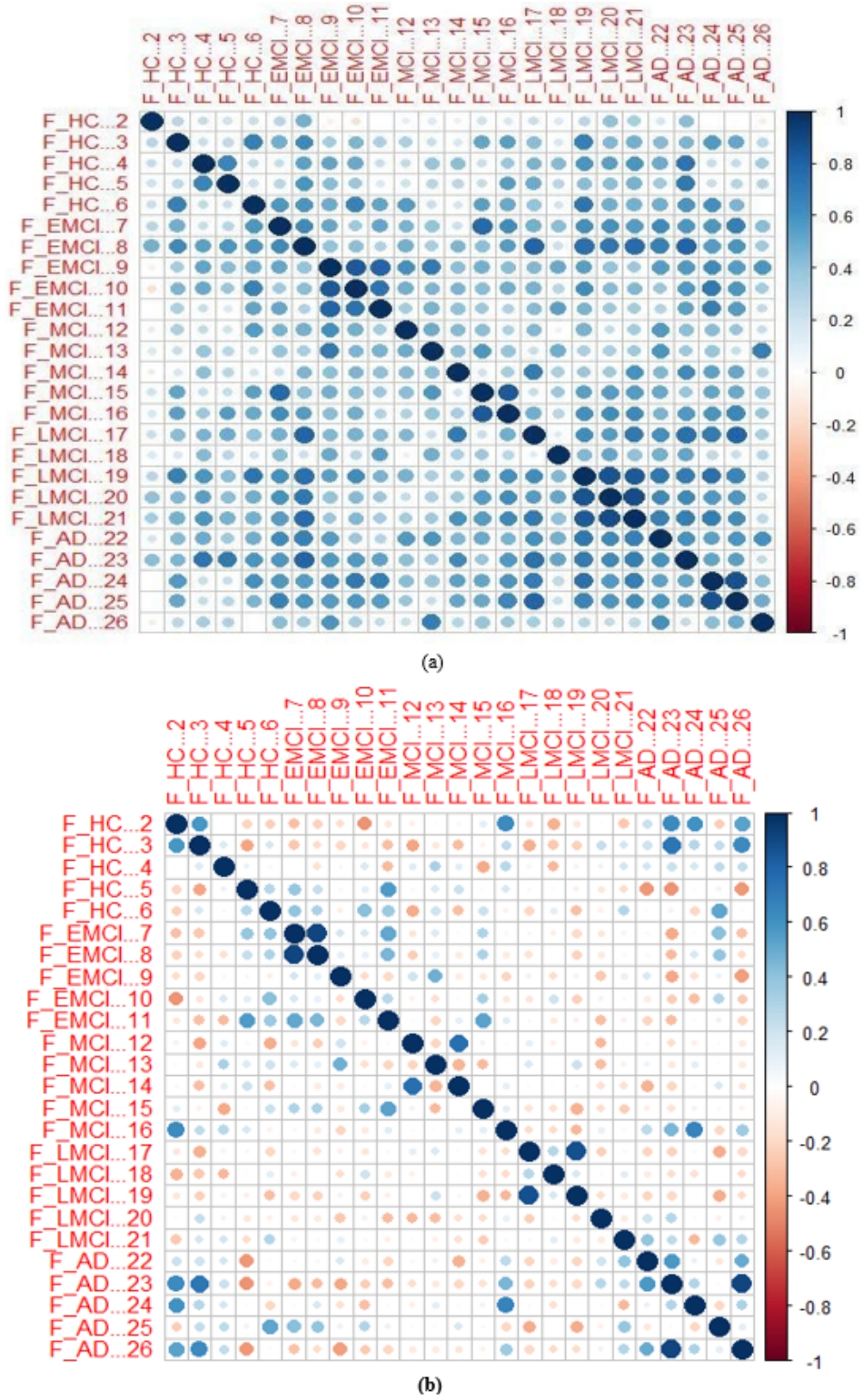

Fig 4. (a) Correlogram plot showing pairwise correlations among the full set of extracted radiomic features. (b) Correlogram plot showing correlations among the representative features selected using the MSRC method

Furthermore, features attained from EMCI, LMCI and HC show highly significant variation in CSF. This indicates the efficacy of MSRC features in discerning the degree of severity.

3.6 Diagnostic and prediction accuracy using SVM classifier

The performance of the considered feature vectors was assessed using a multi-class Support Vector Machine (SVM). To prevent any potential overlap between training and testing data, all image features from the same subject were grouped together and assigned entirely to one dataset. Specifically, 70% of the subjects (and their corresponding image features) were used for training (including 5-fold internal cross-validation), while the remaining 30% were reserved for independent external testing. The internal cross-validation evaluated the model's stability across folds, whereas the external validation assessed its generalization to unseen subjects. This ensured that no slice or feature from the same subject appeared in both datasets, thereby preventing image-level data leakage. Consequently, the external validation accurately reflects model performance on truly unseen subjects.

Initially, classification was performed using individual texture features. These features yielded relatively lower accuracy compared to the fused feature vectors, likely because individual descriptors capture limited morphological variation. When the entire fused feature set was used without feature selection, the model achieved an accuracy of 91.47%, indicating that many features contained redundant or similar information.

Subsequently, feature selection was applied using the MSRC method, which resulted in a classification accuracy of 93.67%. The improved performance suggests that the selected features effectively represent variations in cerebrospinal fluid (CSF) texture associated with Aβ peptide aggregation and neurofibrillary tangles (NFTs) deposition. These features capture subtle CSF texture changes occurring prior to visible degeneration, thereby improving prognostic discrimination.

To further validate the robustness of the proposed features, the model was trained and tested using SVMs with four kernel functions such as Linear, RBF, Polynomial, and Sigmoid in combination with three hyperparameter-tuning strategies: Grid Search, Bayesian Optimization, and Random Search. The search space included the regularization parameter $C \in [0.01, 1]$ and kernel scale $\gamma \in [1, 10]$. Among all configurations, the Linear Random SVM achieved the highest and most stable performance, with a mean cross-validation accuracy of 93.67% and a held-out test accuracy of 92.85%, showing a minimal performance drop between training and testing. Other kernel and tuning combinations achieved accuracies in the 91-92% range, as summarized in Table 3.

Table 3. Classifier performance using various kernels and tuning strategies with 95% confidence intervals

Kernel	Tuning Method	Accuracy (Mean $\pm$ CI)	F1-Score (Mean $\pm$ CI)	Held out Test Accuracy
Linear	Grid	0.9110 ± 0.0120	0.9030 ± 0.0110	0.9100
Linear	Bayes	0.9150 ± 0.0105	0.9070 ± 0.0095	0.9140
Linear	**Random**	$\mathbf{0.9367 \pm 0.0075}$	$\mathbf{0.9350 \pm 0.0080}$	**0.9285**
Polynomial	Grid	0.9100 ± 0.0130	0.9020 ± 0.0120	0.9090
Polynomial	Bayes	0.9140 ± 0.0110	0.9050 ± 0.0105	0.9120
Polynomial	Random	0.9175 ± 0.0090	0.9090 ± 0.0095	0.9150
RBF	Grid	0.9120 ± 0.0130	0.9040 ± 0.0125	0.9110
RBF	Bayes	0.9180 ± 0.0100	0.9090 ± 0.0095	0.9150
RBF	Random	0.9200 ± 0.0085	0.9110 ± 0.0080	0.9165
Sigmoid	Grid	0.2000 ± 0.0000	0.3333 ± 0.0000	0.2000
Sigmoid	Bayes	0.3000 ± 0.0150	0.4000 ± 0.0140	0.3100
Sigmoid	Random	0.2500 ± 0.0100	0.3500 ± 0.0100	0.2600

Although non-linear kernels such as RBF and Polynomial were also tested, their improvements were marginal due to the high-dimensional yet correlated nature of the radiomic features. The linear kernel offered better interpretability in identifying the most discriminative features related to dementia progression, which is advantageous for understanding feature contributions within the CSF region. Furthermore, the MSRC-selected features, obtained through subspace-based ranking and redundancy reduction, effectively transform the complex high-dimensional texture space into a more structured and linearly separable representation. This transformation minimizes feature correlation and enhances the discriminability between classes, enabling the Linear SVM to capture meaningful patterns without requiring non-linear mapping. Consequently, the Linear SVM provides superior generalization and stability while maintaining interpretability. This balance between accuracy, consistency, and transparency supports the selection of the Linear–Random SVM as the optimal model for this study.

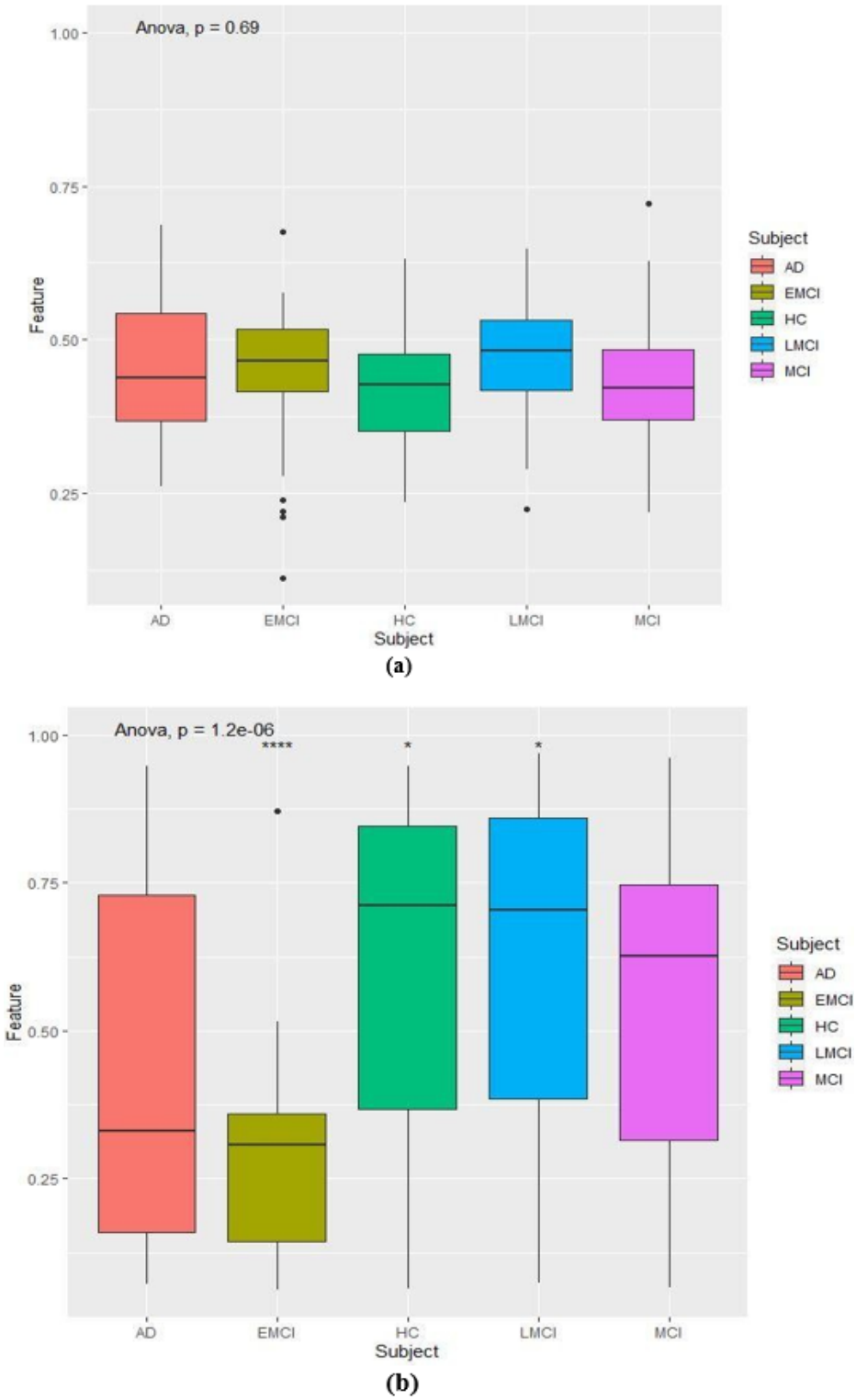

Fig 5. HC and various severity classes performance of CSF texture feature using ANOVA for (a) whole set of feature vector, and (b) MSRC based feature vector

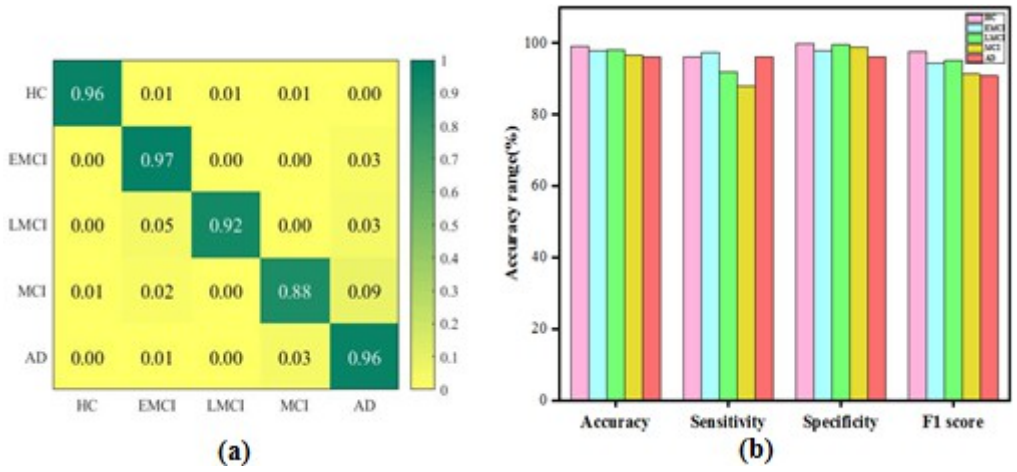

Fig 6. Confusion matrix and classifier performance of MSRC based features

Figure 6(a) shows the confusion matrix for the MSRC-based feature set, demonstrating that CSF-derived features effectively distinguish healthy controls (HC) and severity classes. The misclassification observed in MCI could be attributed to the subtle pathological changes present at that stage. The classification performances for each class are presented in Figure 6(b). The obtained accuracies were 99% for HC, 97% for EMCI, 98% for LMCI, 96% for MCI, and 96.1% for AD, indicating an improved prediction rate across all prognosis stages. The sensitivity values (96%–97% for most classes) show that the classifier reliably detects significant changes in CSF texture features. Similarly, the specificity values 99% (HC), 97% (EMCI), 99% (LMCI), 98% (MCI), and 96% (AD) indicate high discriminative power. The F1-scores of 97%, 94%, 95%, 92%, and 91% for HC, EMCI, LMCI, MCI, and AD, respectively, confirm balanced performance across sensitivity and precision. Figure 7 illustrates the ROC curve, where the area under the curve (AUC) values of 0.999 (HC), 0.995 (EMCI), 0.992 (LMCI), 0.995 (MCI), and 0.989 (AD) demonstrate the reliability of the proposed approach in identifying prognostic differences.

3.7 Effect of MMSE score with significant CSF texture features

The extracted prominent texture features from the CSF regions of HC, EMCI, MCI, LMCI, and AD subjects were correlated with their clinical MMSE scores. The MMSE ranges from 0-30 based on cognitive assessment of a subject. Commonly the score decreases with the progression of cognitive impairment. The *p*-values ($p \approx 0.04$-0.08) were found to be weak to moderate, indicating a modest but consistent relationship between CSF texture variations and cognitive performance across stages. Specifically, HC ($p = 0.083$) and AD ($p = 0.041$) groups showed slightly higher correspondence, suggesting that texture-based features more distinctly capture changes at the extremes of the disease spectrum. MCI ($p = 0.078$) exhibited moderate association, whereas EMCI and LMCI showed marginal significance, likely due to the limited sensitivity of MMSE in these transitional stages.

These findings suggest that the significant CSF features exhibit a mild linear relationship with MMSE and may provide supportive indicators of severity progression. However, given the restricted sensitivity of MMSE and the complexity of cognitive decline, these correlations should be interpreted cautiously and considered indicative rather than conclusive of clinical association. Further validation using multimodal imaging (MRI, fMRI) and complementary clinical scales such as ADAS-Cog and CDR-SB will be essential to enhance the clinical relevance and robustness of the proposed approach.

4 Discussion

Finding and significance from this study

Brain regions such as white matter, grey matter, and cerebrospinal fluid (CSF) play a crucial role in maintaining normal functional activities of the brain. Any alterations, shrinkage, or tissue loss within these regions contribute to neurodegenerative progression. Among them, variations in CSF distribution and texture are often reflective of underlying pathological changes and are strongly associated with dementia prognosis. Characterizing these subtle alterations can therefore facilitate early and preclinical diagnosis.

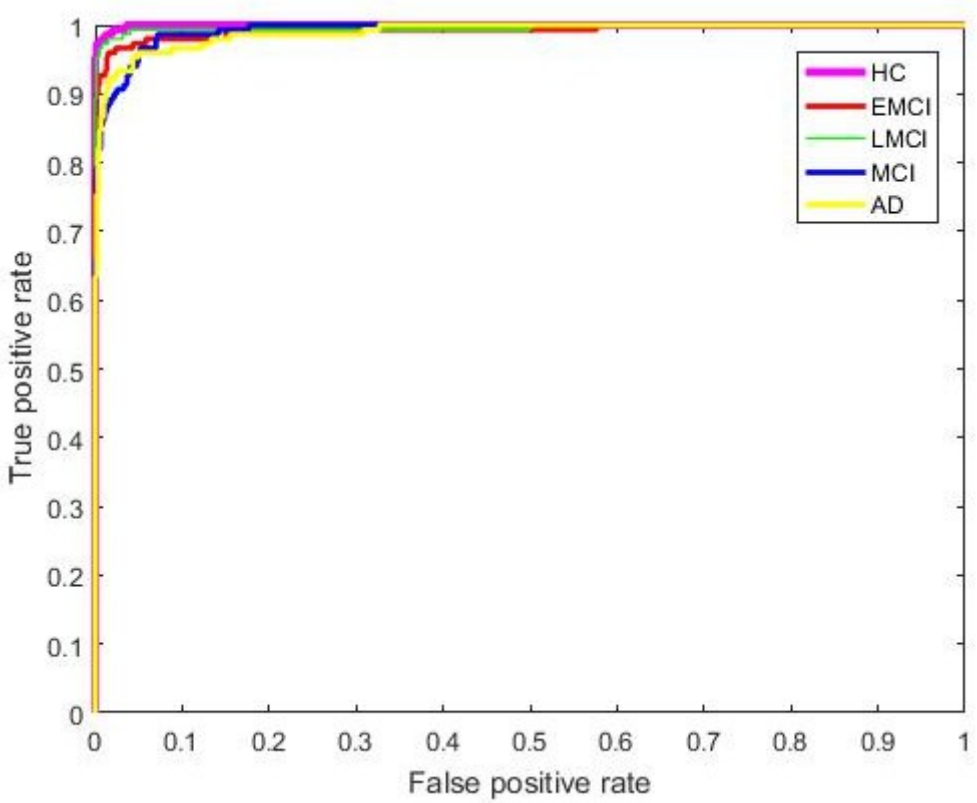

Fig 7. ROC curve for MSRC based features for HC, EMCI, MCI, LMCI and AD

In this study, MR images of HC, EMCI, MCI, LMCI, and AD subjects obtained from the ADNI database were analyzed. Preprocessing using the ROBEX algorithm effectively removed non-brain regions while preserving anatomical boundaries, ensuring accurate CSF delineation for subsequent analysis. To overcome segmentation challenges arising from intensity inhomogeneity, the Multilevel Tsallis Entropy–based Moth Flame Optimization (MFO) method was employed. The adaptive thresholding achieved by MFO enabled reliable delineation of CSF without over- or under-segmentation of neighboring tissues. The robust agreement with the reference standard, as indicated by high Dice and Jaccard indices, confirms that the proposed approach efficiently handles intensity variations and irregular boundaries.

Following segmentation, texture features were extracted from the CSF regions to capture microstructural alterations across severity groups. The combination of GLCM, ST, PHOG, ZM, and LBP descriptors provided a rich representation of spatial patterns and intensity distributions. However, due to the large number of features, a robust selection framework was required to isolate the most discriminative and non-redundant ones.

The Multi-Subspace Randomization and Collaboration (MSRC) framework was adopted for this purpose. Unlike conventional methods that evaluate features in a single space, MSRC explores multiple subspaces and ranks features according to their independent discriminative performance. The correlogram analysis demonstrated that MSRC-selected features exhibited distinct correlation behavior compared to the complete set, indicating their ability to highlight disease-relevant variations. Comparison with benchmark methods such as LASSO, Mutual Information (MI), and Recursive Feature Elimination (RFE) showed that MSRC achieved higher feature stability, as supported by its superior Jaccard Similarity Index. Statistical validation through ANOVA further confirmed that MSRC-selected features significantly differentiated disease stages ($p < 0.05$), particularly in early progression groups such as EMCI and LMCI.

For classification, the selected features were employed in a multiclass Support Vector Machine (SVM) model. The subject-level partitioning ensured unbiased evaluation between training and testing. The results revealed that MSRC-enhanced features improved class separability, with the Linear–Random SVM demonstrating the most stable and interpretable performance. The linear decision boundary indicates that MSRC transformation effectively reduced redundancy and enhanced discriminative

margins between HC and severity classes. Moreover, high specificity across classes suggests that the model accurately excluded non-representative subjects, which is critical for clinical reliability.

Clinical validation was performed by correlating the extracted CSF features with Mini-Mental State Examination (MMSE) scores. Although moderate correlations were observed, the results indicate that texture-derived biomarkers reflect structural and compositional changes in CSF corresponding to cognitive decline trends. This suggests that imaging-derived texture metrics can serve as reliable indicators of disease severity, complementing cognitive assessments.

Overall, the integration of entropy-based segmentation, MSRC-driven feature selection, and multiclass SVM classification forms a coherent and interpretable diagnostic pipeline. The framework demonstrates high accuracy, stability, and generalizability across multiple disease stages. Compared with existing models such as clustering (80%), logistic regression (74.9%), XGBoost (84%), and random forest (75%), the proposed approach achieves superior diagnostic performance while maintaining interpretability and reproducibility as shown in Table 4.

The developed pipeline provides a holistic understanding of CSF variations in dementia. The findings suggest that texture-based CSF features can act as potential biomarkers for distinguishing disease severity. The statistically validated performance and strong cross-stage generalization emphasize the reliability and translational potential of the proposed model.

Table 4. The state of art works carried out on CSF MR images in ADNI Database

References	Techniques	Accuracy
(11)	CSF Features+ clustering Classes- 2	80%
(4)	CSF Features+ cognitive score+ logistic regression model Classes- 2	74.9%
(5)	CSF Features + XGBoost Classes- 2	84%
(12)	CSF+Random Forest Classes- 3	75%
(24)	CSF Features +MRI features +SVM Classes- 2	90.3%
(25)	CSF Features + classification and regression tree Classes- 3	74.65%
(13)	CSF + Imaging Feature+ ApoE genotype + SVM Classes- 2	92.26%
(22)	Neuroimaging markers+ Demographics+ Genetic information (ApoE4) and CSF biomarkers Classes-5	57%
(3)	CSF Features+ Demographics +logistic regression Classes- 2	89.9%
Proposed method	**MFO segmentation+ CSF texture features+ MCFS+ SVM Classes-5**	**93.67%**

5 Conclusion

Traditional MRI biomarkers, such as tissue atrophy and volume loss, are commonly observed in the brains of individuals with dementia. These pathological processes alter water content and diffusion properties, leading to MR signal intensity variations that affect CSF texture. Such variations can reveal subtle changes in intensity distribution, heterogeneity, and spatial patterns associated with disease progression. However, despite their diagnostic potential, CSF characteristics remain underexplored for differentiating dementia stages.

In this study, T1-weighted MR images of HC, EMCI, MCI, LMCI, and AD subjects from the ADNI database were analyzed. The CSF region was segmented using the Multilevel Tsallis Entropy–based Moth Flame Optimization (MFO) method. Texture features were extracted, and the most significant ones were identified using the Multi-Subspace Randomization and Collaboration (MSRC) framework. A multiclass Support Vector Machine (SVM) was employed to classify the variations in CSF texture between healthy and diseased groups. The proposed approach demonstrated robust performance in handling irregular tissue boundaries during segmentation and effectively captured subtle microstructural changes through texture features.

ANOVA confirmed the statistical significance of the selected features, and SVM classification achieved strong differentiation across all groups.

Therefore, the MSRC-selected CSF texture features serve as effective biomarkers for quantifying pathological changes across dementia stages. Finally, these findings highlight the unexplored role of CSF texture as a crucial biomarker, offering a novel perspective in characterizing dementia severity. Future work could expand on these findings by integrating multimodal approaches and explainable deep learning techniques for improved early diagnosis of Alzheimer's Disease.

6 Disclosures

The authors declare no competing interests.

7 Conflict of Interest

The authors have no conflict of Interest.

References

1) Raza HA, Ansari SU, Javed K, et al. A proficient approach for the classification of Alzheimer's disease using a hybridization of machine learning and deep learning. *Sci Rep*. 2024;14(30925):1–14. https://doi.org/10.1038/s41598-024-81563-z.
2) Kimura N, Sasaki K, Masuda T, et al. Machine learning models for dementia screening to classify brain amyloid positivity on positron emission tomography using blood markers and demographic characteristics: a retrospective observational study. *Alz Res Therapy*. 2025;17(25):1–14. https://doi.org/10.1186/s13195-024-01650-1.
3) Dong YF, Jie MJ, Shan H, Wei-Wei L, Shen YY, Zhen W, et al. Establishment of combined diagnostic models of Alzheimer's disease in a Chinese cohort: the Chongqing Ageing & Dementia Study (CADS). *Translational Psychiatry*. 2022;12(252):1–9. https://doi.org/10.1038/s41398-022-02016-7.
4) Valles-Salgado M, Gil-Moreno MJ, Cid REC, Delgado-Álvarez A, Ortega-Madueño I, Delgado-Alonso C, et al. Detection of cerebrospinal fluid biomarkers changes of Alzheimer's disease using a cognitive stress test in persons with subjective cognitive decline and mild cognitive impairment. *Front Psychol*. 2024;26:1–11. https://doi.org/10.3389/fpsyg.2024.1373541.
5) Alexander YG, John PL, Kavita S, Jonghyun B, Keagan B, et al. Machine Learning Classification of Mild Cognitive Impairment using Advanced Multi-Shell Diffusion MRI and CSF Biomarkers. *Medrxiv*. 2025. https://doi.org/10.1101/2025.02.27.25322792.
6) Decaix T, Mouton-Liger F, Dumurgier J, Cognat E, Vrillon A, Hugon J, et al. Usefulness of Cerebrospinal Fluid Alzheimer's disease biomarkers in older patients: Evidence from a national multicenter prospective study. *J Prev Alzheimers Dis*. 2025;12(1):100009. https://doi.org/10.1016/j.tjpad.2024.100009.
7) Ma J, Hu J. An improved particle swarm optimization for multilevel thresholding medical image segmentation. *PLoS One*. 2024;19(12):1–24. https://doi.org/10.1371/journal.
8) Abdul KM, Saurabh C. Modified Moth-Flame Optimization Algorithm-Based Multilevel Minimum Cross Entropy Thresholding for Image Segmentation. *International Journal of Swarm Intelligence Research*. 2020;11(4):1–17. https://doi.org/10.4018/IJSIR.2020100106.
9) Leandrou S, Lamnisos D, Mamais I, Kyriacou PA, Pattichis CS. Assessment of Alzheimer's Disease Based on Texture Analysis of the Entorhinal Cortex. *Front Aging*. 2020;12(176):1–13. https://doi.org/10.3389/fnagi.2020.00176.
10) Huang D, Cai X, Wang CD. Unsupervised feature selection with multi-subspace randomization and collaboration. *Knowl Based Sys*. 2019;182:104856. https://doi.org/10.1016/j.knosys.2019.07.027.
11) Tijms BM, Gobom J. Pathophysiological subtypes of Alzheimer's disease based on cerebrospinal fluid proteomics. *Brain*. 2020;143:3776–3792. https://doi.org/10.1093/brain/awaa325.
12) Matthijs B, Chao-Yi W, Hiroko HD, Shannon NL, Weiwei W, TuKiet L, et al. Machine learning on unbiased proteomics of cerebrospinal fluid uncovers differential molecular signatures of Alzheimer's disease and Normal Pressure Hydrocephalus. *The journal of Alzheimer's Association*. 2025. https://doi.org/10.1002/alz.091783.
13) Nemali A, VockerT N, Berron D, Maas A, Bernal J, Yakupov R, et al. Gaussian Process-based prediction of memory performance and biomarker status in ageing and Alzheimer's disease - A systematic model evaluation. *Med Image Anal*. 2023;90(102913):1–17. https://doi.org/10.1016/j.media.2023.102913.
14) Azam H, Tariq H, Shehzad D, Akbar S, Shah H, Khan ZA. Fully Automated Skull Stripping from Brain Magnetic Resonance Images Using Mask RCNN-Based Deep Learning Neural Networks. *Brain Sci*. 2023;13(9):1255. https://doi.org/10.3390/brainsci13091255.
15) Decaix T, Mouton-Liger F, Dumurgier J, Cognat E, Vrillon A, Hugon J, et al. Usefulness of Cerebrospinal Fluid Alzheimer's disease biomarkers in older patients: Evidence from a national multicenter prospective study. *J Prev Alzheimers Dis*. 2025;12(1):100009. https://doi.org/10.1016/j.tjpad.2024.100009.
16) Jinge S, Yi C, Zhennao C, Ali AH, et al. Multi-threshold image segmentation based on an improved whale optimization algorithm: A case study of Lupus Nephritis. *Biomedical Signal Processing and Control*. 2024;96(106492). https://doi.org/10.1016/j.bspc.2024.106492.
17) Muduli D, Dash R, Majhi B. Automated breast cancer detection in digital mammograms: A moth flame optimization-based ELM approach. *Biomed Signal Process Control*. 2020;59(101912):1–12. https://doi.org/10.1016/j.bspc.2020.101912.
18) Rohini P, Sundar S, Ramakrishnan S. Characterization of Alzheimer conditions in MR images using Volumetric and Sagittal Brainstem Texture features. *Comput Methods Programs Biomed*. 2019;173:143–155. https://doi.org/10.1016/j.cmpb.2019.03.003.
19) Kaplan K, Kaya Y, Kuncan M, Ertunç HM. Brain tumor classification using modified local binary patterns (LBP) feature extraction methods. *Med Hypotheses*. 2020;139(109696):1–12. https://doi.org/10.1016/j.mehy.2020.109696.
20) Muhammad AR, Mohammad RF, Farmadi A, et al. Classification of brain tumor based on shape and texture features and machine learning. *Indonesian J Electronics Electromed Eng Med Inform*. 2024;6(4):240–251. https://doi.org/10.35882/27236g49.
21) Zhang W, Sun C. Corner Detection Using Multi-directional Structure Tensor with Multiple Scales. *Int J Comput Vis*. 2019;128:438–459. https://doi.org/10.1016/j.artmed.2019.05.003.
22) Gupta Y, Lama RK, Kwon GR. Prediction and Classification of Alzheimer's Disease Based on Combined Features from Apolipoprotein-E Genotype, Cerebrospinal Fluid, MR, and FDG-PET Imaging Biomarkers. *Front Comput Neurosci*. 2019;13:1–18. https://doi.org/10.3389/fncom.2019.00072.

23) Yang S, Zhang X, Du X, Yan P, Zhang J, Wang W, et al. Prediction of cognitive conversion within the Alzheimer's disease continuum using deep learning. *Alzheimers Res Ther*. 2025;17(1):41. https://doi.org/10.1186/s13195-025-01686-x.
24) Agnès PM, Bertrand T, Neus F, Sergi B, Beatriz B, Jordi JP, et al. Beyond group classification: Probabilistic differential diagnosis of frontotemporal dementia and Alzheimer's disease with MRI and CSF biomarkers. *Neurobiol Aging*. 2024;144:1–11. https://doi.org/10.1016/j.neurobiolaging.2024.08.008.
25) Alana C, Marcos P, Júlia L, Florindo S, Márcia R, Wagner G, et al. Decision tree-based classification as a support to diagnosis in the Alzheimer's disease continuum using cerebrospinal fluid biomarkers: insights from automated analysis. *Braz J Psychiatry*. 2022;44(4):370–377. https://doi.org/10.47626/1516-4446-2021-2277.